Design, Simulation and Implementation of Brushless DC Motor Drive supplied from Current Source Inverter based on Space Vector Modulation Strategy

PAKSAZ Saeed [1], HALVAEI Niasar Abolfazl[2], ABDOLLAHI Yahya[3]

University of Kashan, Iran,
Department of Electrical & Computer Eng,
Kashan, P.O.Box: 87317-53153, Iran,
[1]spaksaz@gmail.com, [2]halvaei@kashanu.ac.ir, [3]Abdollahi.y@gmail.com,

Abstract *– Today, the brushless DC motors (BLDCs) have been widely used in industry and consumer application due to their unique advantages. These motors are generally supplied from voltage source inverters (VSIs). These inverters have a very simple structure, but have problems such as unwanted short circuit across dc-bus and using bulky capacitor in the dc-bus. Using the current source inverters (CSI) is one of the ways to reduce the mentioned problems in VSI-BLDC motor drives. In this paper, the space vector modulation (SVM) strategy is employed for switching in CSI-BLDC motor drive in order to reduce the switching losses, minimize current and torque ripple and increase the reliability of the drive. The BLDC motor drive model is implemented in the Proteus simulator software and the motor behavior is simulated at different conditions. In order to confirm the simulation results, an experimental setup system is designed and implemented.*

Keywords: *Brushless DC motor, current source inverter, space vector modulation*

I. INTRODUCTION

Over the past two decades, the use of brushless DC motors (BLDCs) have been of great interest due to their advantages such as high efficiency, high torque and power density, simple construction, ease of control, low maintenance cost, simple and cheaper drive system rather than other electrical motors such as synchronous and induction motor (IM). Even with disadvantages such as more torque ripple than PMSM, and also need to the drive even at constant speed, BLDC motors are used in many industrial, household, mass production and high performance applications [1, 2].

Most BLDC motors are supplied through the voltage source inverters (VSIs) that have a simple structure [3]. With the development of power electronics devices as well as development of the high speed digital signal processors, various types of VSIs have been proposed for BLDC motor drives, including unipolar and bipolar two-level inverters, and multi-level inverters [3,4]. Also, various switching strategies have been used in the VSIs of brushless DC motor drives, which include hysteresis current control, space vector modulation, and one-cycle control (OCC) [5]. When using VSI, the conventional method for controlling of BLDC motors (with trapezoidal back-EMF voltage) is injection the rectangular current with a range of 120 degrees in the motor phases, which leads to the constant instantaneous torque. The creation of rectangular currents in the phases can be achieved by various control methods such as DC link current regulation, independent regulation of three-phase current or direct torque control [6]. The using of simple VSI as well as simple proposed control methods leads to a simple and cheap electrical drive (hardware and control system) for these motors.

Despite the simplicity and advantages of VSIs, they suffer from some disadvantages. The main defect of the VSI inverter comes from the short circuit across DC bus, which is due to the unwanted simultaneous connection of the two switches on one leg. Also, the impact of the fast voltage changes (dv/dt) caused by the PWM output voltage results the problems such as aging of winding insulation, leakage current, bearing problems, and undesirable effects of electromagnetic interference (EMI). These issues lower the drive reliability and make acoustic noises in the motor, especially in medium and high power applications. In addition, the hard switching increases the losses and makes it necessary to select the larger heat sink that increases the volume and the price of drive. Another major disadvantage of other VSI inverters is the dangers of using a bulky electrolytic capacitor in the DC bus, which, in some cases, requires more hardware and additional protection and control circuits. From this perspective and in order to increase the reliability, designers are forced to use film capacitors that are more expensive and bulkier than conventional electrolytic capacitors. In terms of control, the undesirable performance of VSI drives is also noticeable for low-inductance permanent magnet brushless motors at high speeds and field-weakening region. Also, the performance of the diodes in reverse current in these drives reduces the power factor and efficiency. The set of reasons above has led researchers to consider the use of CSI [7] and other advanced inverters such as

impedance source inverters (ZSI) in BLDC motor drives [8].

In the CSI many problems of the VSI get less by using an inductor to in series with the inverter. In the CSI, the DC bus protection feature against of short circuit is inherently existent and dv/dt impact of PWM voltage does not exist at all. Also, the lifetime of the inductor is greater than the lifetime of the capacitor and there is no risk of capacitor for the inductor. The CSIs are of great interest in high-power applications of electric drives. The load commutated inverter (LCI) arrangement is one of the most commonly used inverters, which use thyristor devices [9]. But CSIs based on thyristors are suitable for high-power industrial applications and are not suitable for low power motor drives. Lately, more researches have been established on application of CSI drives using of high-speed switches as shown in Fig. 1.

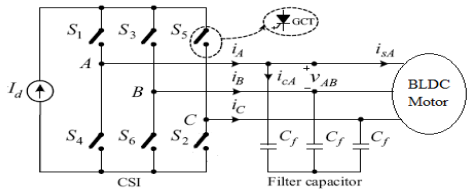

Fig. 1 Current source inverter based brushless DC motor drive

In general, it may not be possible to make an absolute comparison between the advantage of using the CSI or VSI in the BLDC motor drive, and the application is intended to make the use of each one more justifiable. For utilities such as electric vehicles where reliability is important, use of CSI is more reliable [10, 11]. Creating the current source is the main point in the CSI inverters. The simplest solution is to use a series voltage source and an inductor. This structure, despite its simplicity, requires the use a great inductor. Another way to create a current source is to use a buck converter with a smaller inductor, which uses a closed loop control system to adjust the DC link current to desired level. On this way, several researches have been conducted on the use of CSI for drives of BLDC motors. In [7], the CSI based on the buck converter was used to supply of a sensorless BLDC motor drive with six-step current regulation method. Reference [12] has employed a CSI inverter based on thyristor switches to control of BLDC motor in high power electric transportation. Reference [13] also has used a sensorless BLDC motor drive using zero crossing detection of line-to-line voltages, when a CSI based on buck converter as well as six-step current regulation method are employed. In [14], a CSI based dc/dc converter is used to control of a PMSM controlled via field oriented control strategy and sinusoidal PWM switching technique. In [15], the buck converter in the DC link with the PWM switching technique based on one-cycle control strategy has been used for controlling the BLDC motor powered by the CSI. The advantage of the one-cycle control technique is the elimination of the harmonics caused by the use of the hysteresis current controllers. In most BLDC motor drives, based on the CSI mentioned above, either pulse amplitude modulation (PAM) or pulse width modulation (PWM) based on hysteresis controllers are used. This paper uses space vector modulation (SVM or SVPWM) switching technique to improve the BLDC motor drive performance when using a current source inverter. This paper is organized as follows: In section II, various switching strategies in the CSIs are briefly described. Then, in section III, the SVM technique is used for the CSI-based BLDC motor drive. In section IV, the proposed drive system is simulated in Proteus software. In section V, the proposed CSI-based BLDC motor drive is practically implemented and laboratory test results are presented. In the final section, conclusion is explored.

II. SWITCHING STRATEGIES IN THE CURRENT SOURCE INVERTERS

The current source inverters have six switches with gate turn on/off capability, and each switch is in series with the power diode to prevent of negative voltage. The low capacity capacitors between the motor and the inverter, acts as a filter, provide the motor current at the commutation instants. In CSIs, at any instant, only two switches, one in the upper half and the other in the bottom, are conducting the current and the rest of the switches are off. If the switching state of each key is considered as Sm (that is, m = 1... 6), There is the following restriction between the switching states:

$$\begin{cases} S_1 + S_3 + S_5 = 1 \\ S_2 + S_4 + S_6 = 1 \end{cases} \quad (1)$$

So, in the CSI, there are 9 (32) switching states as illustrated in Fig. 2.

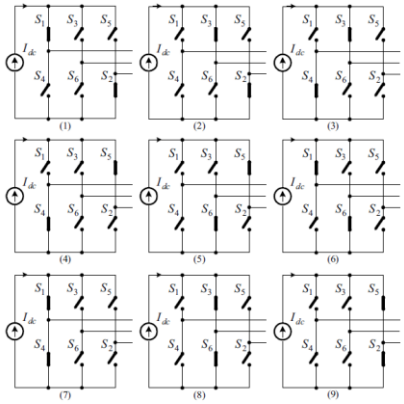

Fig. 2 Switching states in the current source inverter

There are different switching strategies in the CSIs that can be divided into two general categories with switching frequencies equal to fundamental frequency of load (or six-step switching strategy), and PWM switching strategies. The six-step switching strategy is the simplest method that the switches turn off and on during each period of main waveform period (2π) once. The only difference in the six-step switching strategy of the VSI and CSI is that in the VSI, in each instant, three switches are conducting and each switch will be on during π radians, where as in CSI, it is $2\pi/3$ radians and just two switches are conducting [16]. Fig. 3 shows the

command signals of the switches in the six-step switching strategy of CSIs.

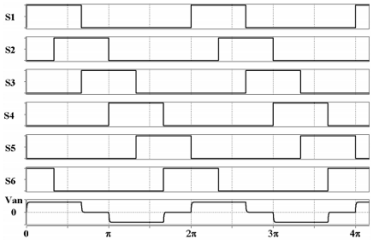

Fig. 3 Switching patterns in the six-step switching strategy of CSI

The six-step switching strategy in CSIs has the same problems of VSIs, which have considerable low-order harmonics that can cause torque ripple. Also, to get the desired current amplitude, it needs to a variable amplitude current source. Hence, PWM switching strategies are preferable to six-step strategy. There are several types of switching methods based on PWM for CSIs; that the trapezoidal PWM method (TPWM) is the basic PWM method. In TPWM method, the triangular signal is compared with the trapezoidal signal and the switching pattern are developed. As shown in Fig. 4, by modulating the first and last 60 degrees of each half cycle, the low-frequency harmonics of the current are minimized. The number of mitigated harmonics is related to the number of pulses per half-period [17]. Here, like the six-step switching technique, the conduction interval is 2π/3 radians. The modulation index here is also defined as the ratio of the reference wave (A) to the carrier wave (Am) amplitude, and the optimum value of the modulation index m is 0.82.

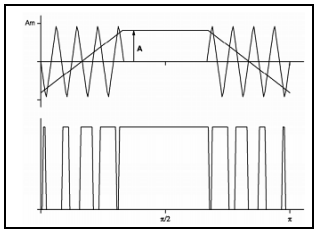

Fig. 4 Switching patterns in the trapezoidal PWM switching strategy of CSI

In order to improve the performance of the CSI inverter, other advanced PWM techniques, such as selected harmonic elimination PWM (SHE-PWM) technique and space vector modulation (SVM), have also been employed. Compared to the two existent techniques of TPWM and SHE-PWM, the SVM technique has more flexibility and faster dynamic response. The SVM technique has recently been used in many applications of electric drive power of induction and synchronous motors. It is expected to be used in future for low power applications and for other types of motors [18]. In this paper, the SVM technique is used to control the CSI and to drive the BLDC motor. As follows, a brief explanation of the theory of SVM technique is explored and then it is used for the BLDC motor drive.

III. SPACE VECTOR MODULATION IN THE CSI

A. Space current vectors

Space vector modulation (SVM) in the CSI is similar to the VSI, with the difference that for VSI, there are 6 active switching states and 2 inactive switching states, but for CSI it has 6 active states (corresponding to the states 1 to 6 in Fig. 2) and 3 inactive states (the states 7 to 9 in Fig. 2) [19]. The reference current vector in the CSI inverter rotates in space at an angular velocity ω and it is defined as:

$$\vec{I}_{ref} = \frac{2}{3}\left(i_A + a i_B + a^2 i_C\right) \quad (a = e^{j120^o}) \\ = I_{ref,\alpha} + jI_{ref,\beta} = \left|\vec{I}_{ref}\right| e^{j\theta} \tag{2}$$

that Iref,α and Iref,β are the length, the real and the imaginary parts of current vector in α-β complex plane respectively. The angle θ is the angular position of current reference vector relative to real axis of the current (α), which can be calculated from the fundamental frequency of inverter output (f1) as:

$$\theta(t) = \int (2\pi f_1) t dt + \theta(0) \tag{3}$$

The line currents consist of discrete values of current, which are Idc, 0, -Idc and on this basis, corresponding to the switching states in Fig. 2, the space current vectors can be shown as vector diagram of Fig. 5. It shows six active current vectors $\vec{I}_1$ to $\vec{I}_6$ and three zero current vectors $\vec{I}_7$ to $\vec{I}_9$ and they form a regular hexagon with six equal sectors, whereas the zero current vectors lie at the center of the hexagon and they can be expressed as:

$$\vec{I}_k = \begin{cases} \frac{2}{\sqrt{3}} I_{dc} e^{j((k-1)\frac{\pi}{3}-\frac{\pi}{6})} & for \;\; k = 1,2,3,4,5,6 \\ 0 & for \;\; k = 7,8,9 \end{cases} \tag{4}$$

The active switches corresponding to each vector are indicated on Fig. 5 that for example on-state switch (S_1,S_2) means S_1 and S_2 are conducting. The space vector modulation technique approximates the current reference vector $\vec{I}_{ref}$ by using the nine space vectors $\vec{I}_k$ (k = 1 to 6). If the current reference vector $\vec{I}_{ref}$ is in the sector *k* (between the arbitrary vectors $\vec{I}_k$ and $\vec{I}_{k+1}$), it can be generated by switching between combined with $\vec{I}_k$, $\vec{I}_{k+1}$, and one of zero vectors ($\vec{I}_7$ to $\vec{I}_9$). The vectors $\vec{I}_7$, $\vec{I}_8$ and $\vec{I}_9$ are respectively corresponding to the states that both switches on the left leg (S_1,S_4), middle leg (S_3,S_6), and right leg (S_5,S_2) leg are conducting.

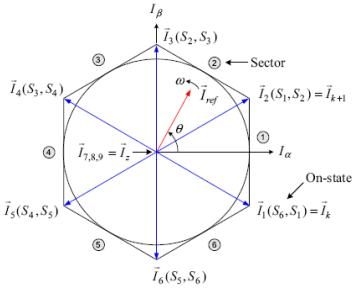

Fig. 5. Definition of the sectors and space vectors in the CSI

B. Dwell time calculation

The dwell time calculation is based on ampere-second balancing principle, that is, the product of current reference vector $\vec{I}_{ref}$ and sampling period T_s equals the sum of current vectors multiplied by the time interval of chosen space vectors. Assuming that the sampling

period T_s is sufficiently small, the current reference vector $\vec{I}_{ref}$ can b ne considered constant during T_s. So, $\vec{I}_{ref}$ can be approximated by two adjacent active vectors $\vec{I}_k$ and $\vec{I}_{k+1}$ and a zero vector $\vec{I}_z$ from the following equation:

$$\vec{I}_{ref}\, T_s = \vec{I}_k\, T_1 + \vec{I}_{k+1} T_2 + \vec{I}_z\, T_0 \qquad (5)$$

Where T1, T2, and T0 are the dwell times corresponding to $\vec{I}_k, \vec{I}_{k+1}, \vec{I}_z$. To ensure that the average of generated current in one sampling period Ts made up of the currents provided by the vectors $\vec{I}_k$, $\vec{I}_{k+1}$, $\vec{I}_z$ used during times T1, T2, and T0 is equal to the current reference vector , the dwell time can be obtained from:

$$\begin{cases} T_1 = mT_s \sin\left(\frac{\pi}{6} - \theta + (k-1)\frac{\pi}{3}\right) \\ T_2 = mT_s \sin\left(\frac{\pi}{6} + \theta - (k-1)\frac{\pi}{3}\right) \\ T_0 = T_s - T_1 - T_2 \end{cases} \qquad (6)$$

That k is the sector number, and m is the modulation index defined as:

$$m = \frac{|\vec{I}_{ref}|}{I_d} = \frac{\hat{I}_{s_1}}{I_d} \qquad (7)$$

where $\hat{I}_{s_1}$ is the peak value of the fundamental frequency component of i_A in Fig. 1. As already mentioned, the zero current vector in each sector is chosen in such a way that a minimum number of switch change occurs. For instance, in sector1,which $\vec{I}_1$ and $\vec{I}_2$ are corresponding to on-state switch (S6,S1) and (S1,S2), the switch S1 is the common. To create the zero current vector, it is better to choose the zero vector $\vec{I}_7$ that includes switch S1 and therefore, switch S1 will be always on during the sampling period Ts.

C. Switching pattern

Using the dwell times obtained by (6), the ampere-seconds in one switching period is kept constant and the fundamental component of the actual current vector will match the reference current vector. However the sequence or pattern of switching affects the THD of output current and device switching loss. There are different switching patterns used to reduce the amount of THD of the output current and switching losses [20]. For example in sector 1, Fig. 6 shows two switching patterns; unsymmetrical and symmetrical. The switching pattern shown in Fig. 6(a) is an unsymmetrical pattern. In order to get the same harmonic performance as the other symmetrical ones, the switching frequency has to be doubled. In this case, the benefits of less switching counts in one switching period cannot be hold. The input current ripple is shown as the red line in Fig. 6. The switching pattern shown in Fig. 6(b) is a symmetrical pattern. Comparing to Fig. 6(a), in the symmetrical pattern, the zero state is split into two parts, one of which is put in the middle, and one of which is put at the side. The peak-to-peak value of the input current ripple changes to half of unsymmetrical. In addition, the ripple frequency is doubled, both of which decreases the size of the passive component, as well as lower the output harmonics. In this paper, the symmetrical pattern shown in Fig. 6(b) is used.

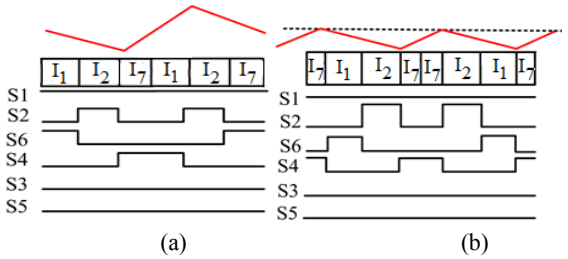

Fig. 6. Two different switching patterns in sector 1(a) unsymmetrical pattern(b) symmetrical pattern

Fig. 7 shows the commands of switches in symmetrical pattern and Table 1 denotes the corresponding switch number in each sector. In the practical implementation of the SVM in the CSI based BLDC motor drive, three references have been designed to generate the correct PWM for CSI and they are proportional to (T_0), (T_0 + T_2), and (T_0 + T_1 + T_2) respectively. The implementation method for symmetrical switching pattern in Fig. 7 is shown in Fig. 8.

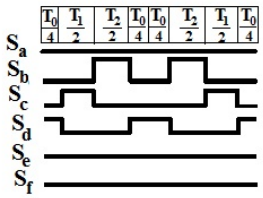

Fig. 7. Switching commands in symmetrical pattern with respect to Table 1

TABLE 1. Corresponding switch numbers in the symmetrical pattern shown in Fig. 7 in each sector

Index \ Sector	1	2	3	4	5	6
a	1	2	3	4	5	6
b	2	3	4	5	6	1
c	6	1	2	3	4	5
d	4	5	6	1	2	3
e	3	4	5	6	1	2
f	5	6	1	2	3	4

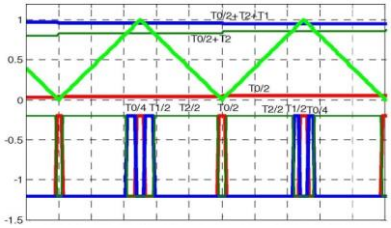

Fig. 8. PWM implementation for symmetrical pattern

IV. SIMULATION OF SVM BASED CSI-BLDC MOTOR DRIVE

The BLDC motor drive system using CSI and based on space vector modulation are implemented with real electronics

devices in Proteus 8 software. Fig. 9 illustrates the schematic diagram of the implemented system. This block diagram consists of a microcontroller type dsPIC33FJ12MC202 made by Microchip, an IC driver, a BLDC motor, start/stop key, and inverter block. The command signals created by the microcontroller and based on SVPWM strategy are shown in Fig. 10 and are applied to six switch drivers and then to the power MOSFET. The patterns A1, A3, and A5 are corresponding to (T0/2), (T1), and (T2). It is observed that at any time only two switches are conducting. The simulation results at low speed 140 rpm and the high speed variation of 250 rpm are shown in Fig. 11.

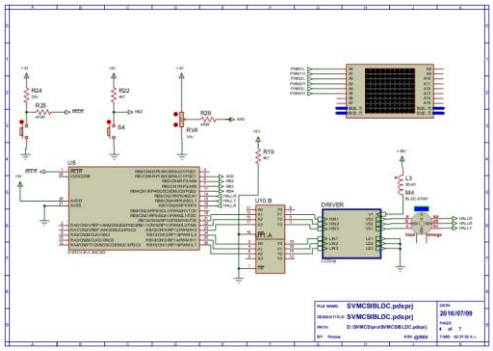

Fig. 9 . Schematic of SVM-based CSI-BLDC motor drive system in Proteus software

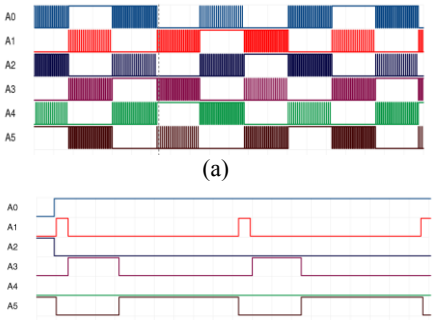

(a)

Fig. 10. Switching patterns in SVM-based CSI-BLDC motor drive system, (a)Command signals to switches (b) The zoom of command signals to switches at the beginning of sector 1

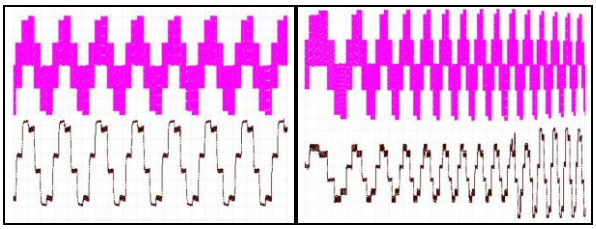

(a) (b)

Fig. 11. Phase voltage and current waveforms in simulation of SVM-based CSI-BLDC motor drive system at speed of 140 rpm (b) transition speed from 140 rpm to 250 rpm

V. IMPLEMENTATION OF SVM-BASED CSI-BLDC MOTOR DRIVE SYSTEM

After ensuring the correct performance of the drive simulated in Proteus, in this section the results of the experimental setup are presented. The schematic of overall block diagram of the system is shown in Fig. 12. In this system, the microprocessor dsPIC33FJ12MC202 is used as controller and IC A3120 as switch driver and buffer. In the power circuit, a 36mH inductor is used to generate the dc current source, and IRF1407 type MOSFET switches. The implemented system is shown in Fig. 13. The BLDC motor is an outer rotor type with power rated 300 W and the non-sinusoidal back-EMF voltage, that its specifications are listed in Table 2.

TABLE 2. Brushless DC motor parameters

Parameter	Value
Rated power	300 [W]
Rated speed	250 [rpm]
Back-EMF voltage constant	0.0666 [V/rpm]
Torque constant	1.25 [N.m/A]
Phase resistance	0.64 [Ω]
Self inductance	1 [mH]
Mutual inductance	0.15 [mH]
Moment of inertia	1.03e-4 [Kgm^2]
Number of poles	16

To apply the mechanical load on this special outer-rotor motor, a belt-spring is designed as shown in Fig. 13. The spring constant value is 2500 N/m. By changing the length of the spring, the amount of torque applied to the motor is adjusted to the desired value. Fig. 14 shows the test results and the waveforms of the motor current at speed of 140 rpm and 250 rpm under load 1 N.m. The filtered voltage waveforms are also illustrated in Fig. 15 at mentioned speed and torque.

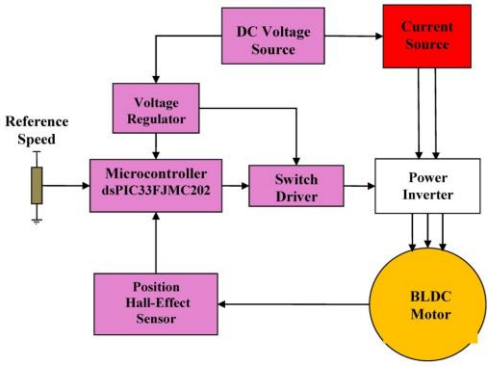

Fig. 12. Schematic of the experimental setup of SVM-based CSI-BLDC motor drive system

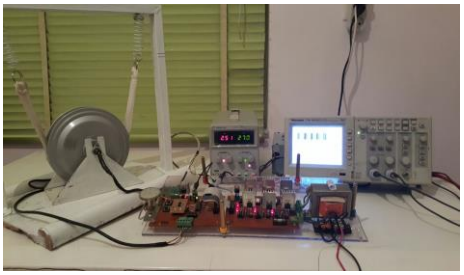

Fig.13 Implemented experimental setup of SVM-based CSI-BLDC motor drive system

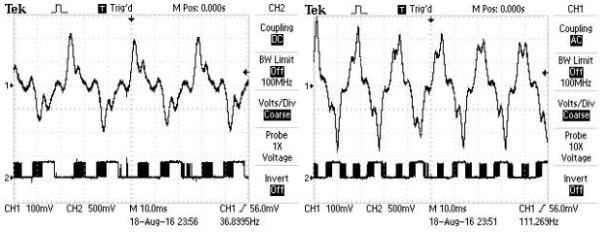

(a) (b)

Fig. 14. Phase current and command to switch S_1 (a) at speed 140 rpm (b) at speed 250 rpm

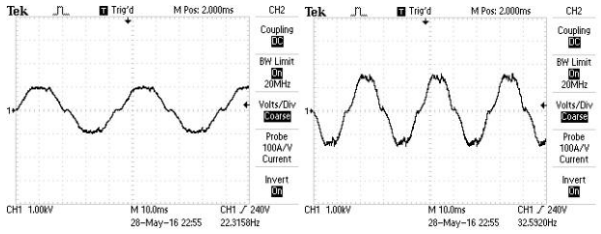

(a) (b)

Fig. 15. The filtered phase voltage at different speeds under torque load 1 N.m at speed 140 rpm (b) at speed 250 rpm

VI. CONCLUSION

In this paper, the performance of BLDC motor drive supplied from CSI using space vector modulation was studied in order to reduce some problems with the use of VSI inverters for these motors. To create the current source, the simple topology of the voltage-source in series with inductor which is suitable for low-power motors was employed. But with increasing the power and current, current stabilization is very difficult and the use of the CSI topology with the buck converter is inevitable. Also, the symmetric switching pattern was used in the CSI space vector modulation for the BLDC motor drive. An actual model in Proteus software was simulated. There is a satisfactory agreement between simulation and experimental results. Many existing microcontroller that are used in drive applications, have complementary output PWM ports with adjustable dead time unit. This feature is put to protect the short circuit across the dc bus through two switches on one leg. But in CSI, to create the zero current vectors, it is need to energize both switches of on the one leg. This problem should be solved with programming technique.

REFERENCES

[1] R. Krishnan, "Permanent Magnet Synchronous and Brushless DC Motor Drives", London: CRC Press, 2010.

[2] A. Halvaei Niasar, A. Vahedi, H. Moghbelli, "Low Cost Sensorless Control of Four-Switch, Brushless DC Motor Drive with Direct Back EMF Detection", Journal of Zhejiang University, Science-A (JZUS), Vol. 10, No. 2, pp. 201-208, October 2009.

[3] S. R. Misal, N. R. Bhasme, "A review of multi-switch BLDC motor drive", IEEE conference on Innovations in Power and Advanced Computing Technologies (i-PACT), pp. 1-7, 2017.

[4] B. S. Kalyani, V. Ma. Mukkavilli, G. Naik, "Performance Enhancement of Permanent Magnet Brushless DC Motor Using Multilevel Inverter", IEEE 7th International Advance Computing Conference (IACC), pp.472-476, 2017.

[5] A. Halvaei Niasar, E. Boloor Kashani, "Implementation of a Novel Brushless DC Motor Drive based on One-Cycle Control Strategy", Iranian Journal of Electrical and Electronic Engineering, Vol.10, No. 3, pp. 244-249, 2014.

[6] Florin Dumitrache, Mihai Romanca, Gheorghe Pana, "Methods for optimizing BLDC motors performance by using different control schemes", International Conference on Optimization of Electrical and Electronic Equipment (OPTIM) & Intl Aegean Conference on Electrical Machines and Power Electronics (ACEMP), pp. 687-69, 2017.

[7] H.C. Chen, H. H. Huang, "Design of buck-type current source inverter fed brushless DC motor drive and its application to position sensorless control with square-wave current", IET Electric Power Applications, Vol. 7, No. 5, pp. 416-426, 2013.

[8] P.C. Loh, "Buck–boost thyristor-based PWM current-source inverter", IEE Proc.-Electr. Power Appl., Vol. 153, No. 5, pp. 664-672, 2006.

[9] M. Pandi Maharajan, P. Muthu, M. Palpandian, S. Kannadasan, "Analysis of low harmonics and high efficient BLDC motor drive system for automotive application", International Conference on Recent Advancements in Electrical, Electronics and Control Engineering, pp. 526-531, 2011.

[10] S. Yongsug, J. Steinke and P. Steimer, "Efficiency comparison of voltage source and current source drive system for medium voltage applications", IEEE Proceedings Power Electronics and Applications, pp.11; 2005.

[11] J. Karthikeyan, R. D. Sekaran, "DC-DC converter CSI fed BLDC motor for defence applications", International Conference on Recent Advancements in Electrical, Electronics and Control Engineering, pp. 68-72, 2011.

[12] J. Wang, L. B. Zhou, G. L. Tao, "Design and Analysis of a Multiphase Permanent Magnet Brushless DC Motor Drive System for High Power Applications", 2nd IEEE Conference on Industrial Electronics and Applications, pp.1182-1187, 2007.

[13] Hung-Chi Chen, and Hung-He Huang; "Speed Control for Buck-Type Current Source Inverter Fed BDCM without Position Sensors", IEEE International Symposium on Industrial Electronics, pp. 1-6, 2013.

[14] L. Tang, G.J. Su, "Boost mode test of a current-source-inverter-fed permanent magnet synchronous motor drive for automotive applications", Control Model. Power Electron. (COMPEL), pp. 1–8, 2010.

[15] O. Mohammadpour, A. Halvaei Niasar, "One Cycle Control of Buck-Type, Current Source Inverter-Fed, Brushless DC Motor Drive", in Proceedings of the 6th IEEE Power Electronics, Drive Systems & Technologies Conference (PEDSTC), pp. 113-118, 2015.

[16] G. Moschopoulos, G. Joos, P. D. Ziogas, "Input characteristics of variable modulation current source inverters", IEEE Industrial Electronics, Control and Instrumentation (IECON), pp. 204-209, 1991.

[17] F. Hinrichsen, I. Koch, W.R. Canders, "Current source IGBT-inverter for low inductive synchronous machines", in the IEEE 35th Power Electronics Specialists Conference 2004 (PESC), Vol. 4, pp.2849-2853, 2004.

[18] Ming-Fa Tsai, Ti-Chung Lee, Chung-Shi Tseng, Wei-Syuan Syu, Yu-Yuan Chen, Wen-Yang Peng, "Vector control of current source inverter-fed axial-flux permanent magnet motors with space vector pulse width modulation", 23rd IEEE International Symposium on Industrial Electronics (ISIE), pp. 920-925, 2014.

[19] D.C. Pham, S. Huang, K. Huang, "Modeling and simulation of current source inverters with space vector modulation", IEEE International Conference on Electrical Machines and Systems (ICEMS), pp. 320-325, 2010.

[20] Q. Lei, B. Wang, F. Z. Peng, "Unified space vector PWM control for current source inverter", IEEE Energy Conversion Congress and Exposition (ECCE), pp. 4696-4702, 2012.